Supporting Information

Ghosh and O'Connor 10.1073/pnas.1319116111

SI Results and Discussion

High Sugar Content and Acidity of Cornmeal Food Leads to Lethality of *dawdle* Mutants. In addition to yeast paste food (YPF), a semidefined food consisting of 5% yeast and 5% dextrose (5y5s), could also rescue viability of *dawdle* (*daw*) mutant larvae (Figs. S2 *B* and *C* and S3*A*). We found that both YPF and 5y5s food was significantly lower in total carbohydrate content compared with cornmeal food (CMF) (Fig. S2*A*). Because *daw* mutants showed defects in sugar homeostasis, we tested whether higher carbohydrate content of CMF is poisonous to the *daw* mutants by challenging them with a high-sugar diet (HSD) (or 5y15s food). HSD caused a small but significant decrease in the viability of the *daw* mutants compared with control larvae (Fig. S3*A*). HSD has been shown to induce peripheral insulin resistance in *Drosophila* larvae (1) and this effect, in combination with impaired insulin release already present in the *daw* mutants, could lead to larval lethality by impairing growth and nutrient availability.

We also examined the effect of acidic food conditions on the viability of *daw* mutants both because *daw* mutant larvae show internal acidosis and because CMF is more acidic (pH 4.3 compared with ~ pH 6.8 of 5y5s food) owing to the addition of propionic acid (PA) as a mold inhibitor. Acidification of food (pH 4.3) with either organic or inorganic acids caused a significant decrease in the viability of *daw* mutants and also caused significant developmental delay (Figs. S2*B* and S3 *B* and *C*). Notably, acidification of food with PA most severely affected larval viability and developmental delay (Fig. S3*B*). We hypothesized that acidic food conditions lead to larval lethality and developmental delay by aggravating the already acidic internal pH of the *daw* mutant larvae. Consistent with this view, we found that transferring *daw* mutant larvae to acidic food conditions caused significant aggravation of the acidosis observed on YPF (Fig. S3*E*). Interestingly, heterozygous mutants also showed a significant but intermediate drop in hemolymph pH compared with wild-type controls, signifying a dose-dependent role of Daw in regulating the acidosis phenotype (Fig. S3*E*).

Alterations in pH homeostasis can have widespread physiological and behavioral consequences, such as muscle degeneration, altered enzymatic activity, and habitat and food choice (2). Predictably, an acidic environment is expected to have a more severe impact on the *daw* mutants, and we did see a severe increase in the lethality of the mutants on acidic food. Preferential vulnerability of the *daw* mutants to PA is intriguing and could be caused by systemic accumulation of the propionate ion that may be more difficult to pump out compared with Cl^- ions. Alternatively, propionate, being hydrophobic, may enter the cells more readily than Cl^- ions and thereby cause more physiological damage. The effect of acidic food on developmental timing can possibly be caused by changes in hormonal signals. In support of this possibility, studies using honey bees and locusts have shown that changing partial pressure of CO_2 affects juvenile hormone levels, and the effects could be mediated by changes in pH (3, 4). Additionally, acidosis has been shown in vertebrates to affect secretion and/or activation of several hormones including corticosteroids, thyroid hormone, and parathyroid hormone (5, 6).

Combining a HSD with PA-acidified food (pH 4.3) resulted in the most severe larval lethality, phenocopying the extent of lethality seen on CMF (less than 10% viability; Fig. S3*C*). Notably, a number of other food conditions that mimicked CMF in nutritional content, or represented extremes of nutritional conditions, did not significantly affect viability of *daw* mutants (Fig. S2 *C* and *D*). Thus, we conclude that lethality of daw mutants on CMF is primarily caused by the high carbohydrate content and PA induced acidity of the CMF.

SI Materials and Methods

Fly Strains. The following fly lines were generated in the laboratory using standard recombination techniques.

daw^1,UAS-dilp2/CyoYFP	*daw^{11},UAS-babo^{CA}/CyoGFP*	*daw^{11},fb-Gal4/CyoGFP*
daw^{11},cg-Gal4/CyoGFP	*daw^{11},mef2-Gal4/CyoGFP*	*daw^{11},OK72-Gal4/CyoGFP*
daw^{11},npc1b1-Gal4/CyoGFP	*daw^{11},Kurs6-Gal4/CyoGFP*	*daw^{11},dilp2-Gal4/CyoGFP*

Foods Used. ***YPF.*** Yeast paste (60%; wt/vol) in water was dabbed on to a soft apple juice agar plate [0.7% *Drosophila* agar (US Biological) and 1× apple juice concentrate (Nature's Nectar)].
CMF. Standard Bloomington food (2.2×) that was prepared in the laboratory was used.

Nutritional Analysis of Food. Analysis of nutrient content of CMF was performed by Medallion Laboratories. Contribution of yeast to nutrient content was calculated from nutrition facts per gram of yeast provided by the manufacturer (Saf-instant; Lesaffre Yeast).

Semidefined Food. All semidefined food contained yeast and dextrose in proportions mentioned (wt/vol), along with 1% (wt/vol) *Drosophila* agar. Semidefined food was boiled for 5 min to heat-inactivate live yeast and poured in vials after cooling them down to about 40 °C.

Generation of Larval Developmental Growth Curve and Larval Growth Conditions. Approximately 150 virgin females and 100 males were crossed in 100-mL volume cages. The crosses were maintained in a 25 °C incubator with a 12-h light/dark cycle and 60% humidity. On day 3 after starting the cross, egg collections were done every day for the next 4–5 d between 1100 hours and 1400 hours (3 h). Larvae hatching from the first collection of eggs were used for generating larval developmental growth curve and subsequent collections were used for relevant experiments. Twenty-four hours post-egg lay, first-instar larvae were transferred to plates of YPF (three plates for each genotype and 30 larvae per plate). The larvae were grown at 25 °C, 60% humidity, and 12-h light/dark cycle, same as the conditions in which crosses were maintained. On day 4 after egg collection, plates were checked every 1–2 h, and the number of pupae, if any, was counted. The time point at which a total of 20–25 pupae have formed was considered 25% pupariation time and a time point (experimental time point) 24 h before this time point was used for the processing of samples arising from subsequent egg collections of that genotype. This process was followed every time a new egg collection cage was set up for an experiment and for every egg collection cage (genotype). When grown on YPF solid plate lids were changed with meshed lids at the end of day 3 after egg lay to avoid excess moisture buildup. Excess moisture in plates tend to seal off air supply and causes larvae to wander prematurely. While generating developmental timing curves on semidefined food, we used the same methodology except 60 larvae were used per vial to allow easy churning of the food.

Triacylglycerol Assay. Samples were prepared by homogenizing three mid–third-instar larvae per sample in 250 μL of ice cold PBT (PBS plus 0.1% tritonX-100). Homogenization was performed in microcentrifuge tubes using a plastic pestle and hand held motor. Subsequently, samples were sonicated (on ice) for 4 s with a 0.5-s pulse at 20% amplitude setting; 10 μL of homogenate was mixed with 200 μL of triglyceride reagent, and the mixture was incubated at room temperature for 15 min. Samples were centrifuged briefly to get rid of any particulate material, and supernatants were transferred to 1-mL disposable cuvettes; 800 μL of free glycerol reagent was added to each sample and incubated at room temperature for 15 min to allow development of color. Spectrophotometric measurements were performed at 540 nm. Triacylglycerol (TAG) content was calculated from TAG standard curves generated with each experiment according to the manufacturer's instructions. Protein estimation was performed using BCA kit using the sonicated samples and ratio of total TAG content to total protein content was reported as normalized TAG content.

Glycogen Assay. Samples were prepared by homogenizing three to four mid–third-instar larvae per sample in 100 μL of ice-cold PBS. Samples were subsequently centrifuged at 2,500 × *g* for 1 min at 4 °C, and supernatant was transferred to 0.2-mL PCR tubes; 10–20 μL of each sample was preserved for protein assay. The remaining supernatants were heat treated at 70 °C for 5 min using a thermocycler. Subsequently, samples were immediately chilled on ice. Protein aggregates were separated by centrifugation (16,000 × *g* for 10 min at 4 °C), and supernatants were used for glycogen estimation. For estimation of total glucose plus glycogen content, 30 μL of the prepared supernatant was incubated with 100 μL of glucose oxidase/peroxidase reagent (Sigma Glucose assay kit; GAGO 20) containing amyloglycosidase (1 μL/mL of glucose reagent; Sigma; A1602-25MG) for 30 min at 37 °C. In parallel, 30 μL of supernatant was incubated with glucose oxidase/peroxidase reagent alone in identical conditions to estimate for total glucose content. At the end of the incubation period, reactions were terminated by adding 100 μL of H_2SO_4 and left at room temperature for 5 min for color to develop. OD was measured at 555 nm, and metabolite contents were calculated from glucose/glycogen standard curved generated along with every experiment. Total glycogen content was determined by subtracting total glucose content from glucose plus glycogen content. Measurements were normalized to total protein estimated with a BCA kit.

Hemolymph Glucose Plus Trehalose Concentration. For each sample, five to six mid–third-instar larvae were washed in PBS and dabbed on kim wipes. Larvae were then quickly ripped open on a piece of parafilm under the dissecting microscope; 1.5–2 μL of hemolymph was carefully collected from this heap of dissected animals using a 2-μL pipettor (P2) and placed on the parafilm to form a small drop; 1 μL of hemolymph was subsequently pipetted out of this drop to 19 μL of trehalase buffer in 0.5 mL tubes, mixed by tapping, and stored on ice while more samples are being collected. This two-step pipetting prevents inadvertent pipetting errors caused by larval tissues clogging the pipette tip. The samples were then centrifuged briefly (3 min at 16,000 × *g*), and supernatants were transferred to 0.2-mL PCR tubes. Samples were heat treated at 70 °C for 5 min in a thermocycler and immediately chilled on ice. Protein aggregates were separated by centrifugation at 16,000 × *g* for 12 min at 4 °C. Supernatants were transferred to new tubes and used for sugar estimation. For sugar (glucose plus trehalose) estimation 2 μL of sample was added to 28 μL of threhalase buffer containing *x* units per milliliter of porcine trehalase, and the mixtures were incubated at 37 °C (water bath) for 16–18 h to convert trehalose to glucose. Subsequently, total glucose concentration was measured using the sigma glucose oxidase kit as mentioned above. Standard curves were generated with every experiment using 1 mg/mL trehalose stock and were used to calculate sugar concentration in the hemolymph.

Hemolymph pH Assay. For hemolymph pH measurement, 3 μL of hemolymph was extracted from a collection of 10–12 mid–third-instar animals and mixed with 2 μL of pyranine dye (Invitrogen; 1.2 mM final concentration). The mixture was briefly centrifuged, and the absorbance spectrum of the supernatant was measured using a multichannel nanodrop spectrophotometer (NanoDrop 8000). The ratio of absorbance at 450 and 405 nm was plotted against a standard curve (curve fitting done using a second degree polynomial equation in excel keeping pH on the *y* axis) to determine the pH. pH standards ranging between pH 6.6 and pH 7.6 were prepared by titrating 50 mM Tris·HCl. Samples were maintained on ice or 4 °C until measurements were made on the nanodrop to avoid any oxidation of phenolic compounds.

Fluorescence Quantification. Confocal Z series of the IPCs were obtained using a 1-μm step size and identical laser power and scan settings. Zeiss Zen software was used to generate multiple intensity projection images. Subsequently, background signal was subtracted and fluorescence intensity was measured by drawing selections on the IPCs.

Quantitative PCR. Tissues dissected from mid-third instar larvae were flash-frozen on dry-ice. Total RNA was extracted using QIAGEN RNeasy Tissue Mini Kit. cDNA prepared using Invitrogen SuperScript III kit and qPCR performed using Roche SYBR green reagent as per instructions (Roche LightCycler 480 Real-Time PCR system). *rpl23* was used as a reference gene for normalization. Primers were designed specifically for qPCR using Primer3 (http://frodo.wi.mit.edu).

Western Blots. Fat body (FB) or muscle/epidermis from six mid-third instar larvae were dissected and homogenized in 50 μL of 1.5× reducing samples buffer. The samples were heated for 10 min, centrifuged, and 10–15 μL of sample was loaded and run on Invitrogen precasted 4–15% 12-well gels. Protein bands were transferred to PVDF membranes and probed using ECL method according to standard protocol. The following primary and secondary antibodies were used at the mentioned dilutions: anti–p-Smad2 1/1000 (Cell signaling), *Drosophila* anti-pAkt S505 1/1000 (Cell Signaling), Pierce goat anti-mouse HRP and goat anti-rabbit HRP at 1/10,000 dilution.

1. Musselman LP, et al. (2011) A high-sugar diet produces obesity and insulin resistance in wild-type *Drosophila*. *Dis Model Mech* 4(6):842–849.
2. Harrison JF (2001) Insect acid-base physiology. *Annu Rev Entomol* 46:221–250.
3. Bühler A, Lanzrein B, Wille H (1983) Influence of temperature and carbon dioxide concentration on juvenile hormone titre and dependent parameters of adult worker honey bees (Apis mellifera L.). *J Insect Physiol* 29(12):885–893.
4. Fuzeau-Braesch S, Nicolas G, Baehr JC (1982) A study of hormonal levels of the locust *Locusta migratoria* cinerascens artificially changed to the solitary state by a chronic CO_2 treatment of one minute per day. *Comp Biochem Physiol A* 71: 53–58.
5. Wiederkehr MR, Kalogiros J, Krapf R (2004) Correction of metabolic acidosis improves thyroid and growth hormone axes in haemodialysis patients. *Nephrol Dial Transplant* 19(5):1190–1197.
6. Mitch WE (2006) Metabolic and clinical consequences of metabolic acidosis. *J Nephrol* 19(Suppl 9):S70–S75.

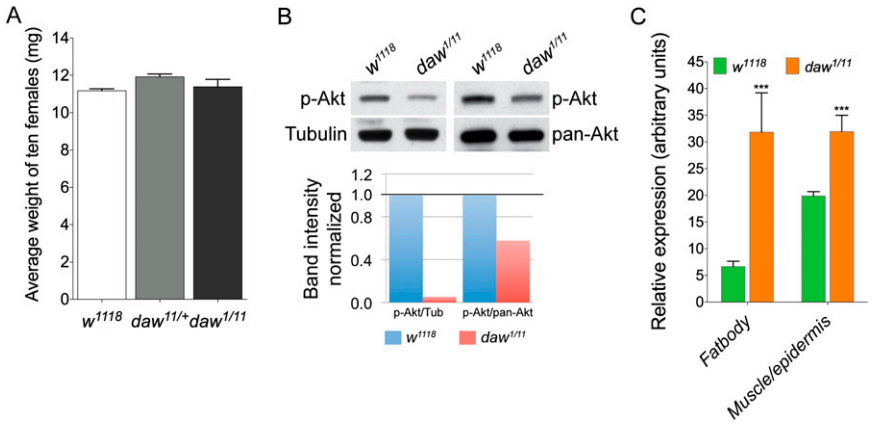

Fig. S1. (*A*) *daw* mutants when grown on YPF reached adult stages and eclosed as adults. The weight of adults after 24 h of eclosion is shown here and mutants were similar in size to both w^{1118} and $daw^{11/+}$ heterozygous controls. Error bars represent ± SEM (n = 5–8 samples each containing 10 healthy virgin females). (*B*) p-Akt level in *daw* mutant and control larval FB shown using Western blot. Results from two independent experiments using either tubulin or pan-Akt as loading control are shown. Quantification of band intensities showed a strong reduction in p-Akt levels in the mutant FB compared with control. (*C*) InR mRNA in *daw* mutant and control FB and muscle was determined using quantitative RT-PCR. *daw* mutants showed a significant increase in expression of InR in both these tissues (n = 6). Error bars represent ± SEM.

A

Nutrient	% in CMF	% in YPF	% in 5y/5s
Lipid	0.1	2.57	0.21
Carbohydrate	18.4	14.1	6.18
Protein	1.76	21.43	1.78
Free Sugar	5.43	0	5

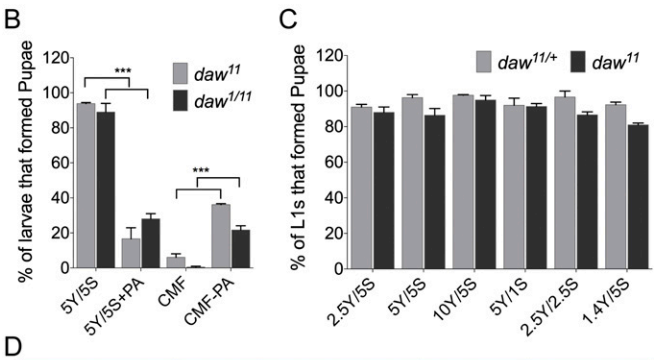

D

Food/Nutrition % mass	Lipid	Carbohydrate	Protein	Free Sugar
CMF	0.1	18.4	1.76	5.43
2.5Y/5S	0.1	3.09	0.89	5
5Y/5S	0.21	6.18	1.78	5
10Y/5S	0.42	12.36	3.5	5
5Y/1S	0.21	6.18	1.78	1
2.5Y/2.5S	0.1	3.09	0.89	2.5
1.4Y/5S	0.06	1.73	0.5	5

Fig. S2. Viability of *daw* mutants on a variety of food conditions that mimic nutritional content of CMF was assayed. (*A*) Comparison of nutritional content of CMF, YPF, and 5y5s food shown as percentage by weight. (*B*) PA used in CMF as a mold inhibitor is toxic to *daw* mutants. Addition of PA to 5y5s food significantly increases lethality of both homozygous and transheterozygous *daw* mutants. Consistently, removing PA from CMF can significantly improve viability of *daw* mutants on CMF. (*C*) A range of food conditions mimicking the major nutrient content of CMF and representing extremes of nutritional conditions has no effect on viability of *daw* mutants compared with controls. (*D*) Nutritional content of the various food conditions on which we checked viability of *daw* mutants. The first four conditions from the top are similar in total free sugar content to CMF. The 1.4Y/5S, 2.5Y/5S, and 5Y/5S food are similar in total yeast, lipid, and protein content compared with CMF, respectively. The 1.4Y/5S food also represents a nutritionally poor diet and the 5Y/1S food represents a high protein low sugar food condition. Error bars represent ± SEM. All viability assays consisted of six independent viability assays each consisting of 60 animals.

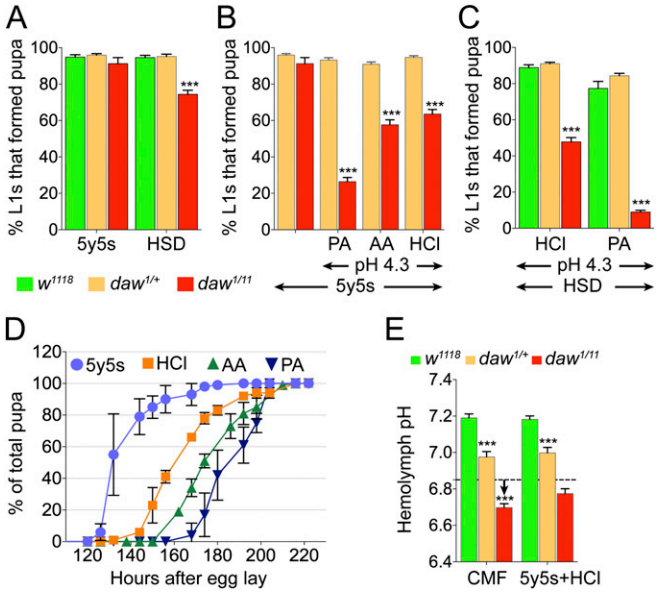

Fig. S3. Effect of high sugar and acidic food conditions on viability of *daw* mutants. (*A*) Viability of *daw* mutant and control larvae on 5y5s and HSD (5y15s) food ($n = 6$). (*B*) Viability of *daw* mutant and control larvae on 5y5s food and 5y5s food acidified with PA, acetic acid (AA) or HCl ($n = 6$). (*C*) Viability of *daw* mutant and control larvae on HSD acidified with HCl or PA ($n = 6$). (*D*) Effect of non acidic and PA-, AA-, and HCl-acidified 5y5s food on timing of pupariation of *daw* mutants compared ($n = 6$). (*E*) Effect on acidic environment on the internal pH of *daw* mutants compared with nonacidic YPF ($n = 8$–12) (dashed line, hemolymph pH of *daw* mutants on YPF). All results are reported as means ± SEM. All viability assays contained 60 animals per sample.

A

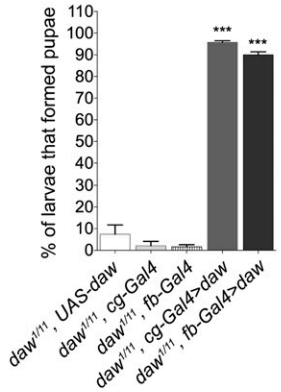

B

Crosses	Observed #		Observed %		Total number of Flies
	Cyo	*Non-Cyo*	*Cyo*	*Non-Cyo*	
daw^{1}/Cyo; UAS-daw X *daw*^{11}/Cyo	466	0	100	0	466
daw^{1}/Cyo; UAS-daw X *daw*^{11}, *dIlp2-Gal4*/Cyo	372	176	74.7	25.3	498
daw^{1}/Cyo; UAS-daw X *daw*^{11}, *OK72-Gal4*/Cyo	502	250	66.76	33.24	752
daw^{1}/Cyo; UAS-daw X *daw*^{11}/Cyo; *mef2-Gal4*	349	125	73.63	26.37	474

Shown is the number (#) and percentage (%) of Cyo and Non-Cyo flies derived from control and *daw*-rescue crosses reared on CMF. Non-Cyo flies are *daw* mutants whereas Cyo flies are heterozygous controls. Expected ratio of Cyo:Non-Cyo for each cross is 2:1

C

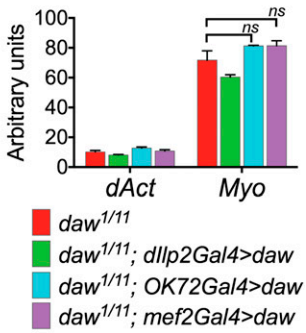

Fig. S4. (*A*) *UAS-daw* construct was overexpressed in the *daw* mutant background using fat body-specific *cg-Gal4* or *fb-Gal4* drivers, and its ability to rescue lethality on CMF was assayed. Overexpression of *daw* using either driver was able to completely rescue viability of *daw* mutants on CMF. Error bars represent ± SEM. All viability assays consisted of 6 independent viability assays each consisting of 60 animals. (*B*) Overexpression of *daw* in the IPCs (*dIlp2-Gal4*), oenocytes (*OK72-Gal4*), or muscle (*mef2-Gal4*) of *daw* mutants was able to rescue viability of daw mutants on CMF all of the way to adult stages. (*C*) Overexpression of *daw* in the IPCs (*dIlp2-Gal4*), oenocytes (*OK72-Gal4*), or muscle (*mef2-Gal4*) of *daw* mutants did not significantly increase expression of *dAct* or *myo* in these mutants ($n = 6$). Expression measured using quantitative PCR and mRNA levels relative to abundance of rPl23 is presented. ns, not significant.

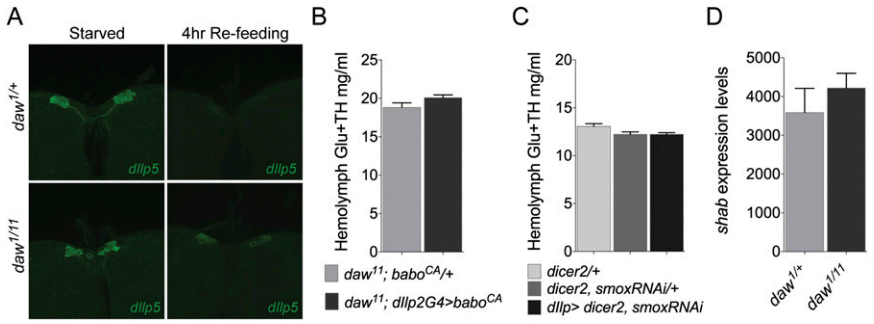

Fig. S5. Daw regulates Dilp release in response to food but may not act directly on the IPCs. (*A*) CNSs dissected from 16-h starved and 4-h refed control and mutant larvae were stained with anti-Dilp5 antibody (green). Under identical staining and imaging conditions, Dilp5 staining was much stronger in mutant refed CNSs than control animals. Dilp5 staining in starved mutant and control animals was identical. (*B* and *C*) Three lines of observations indicate that *daw* regulates IIS in a cell nonautonomous manner. (*B*) $babo^{CA}$ overexpression in the IPCs of *daw* mutants was not able to rescue the diabetic phenotype of *daw* mutants ($n = 12$). (*C*) *SmoxRNAi* along with *dicer2* overexpression in the IPCs was not able to induce a diabetic phenotype in w^{1118} larvae ($n = 14$). (*D*) Expression level of *Drosophila exp-2* homolog *shab* in larval CNSs of *daw* mutants and controls was measured using quantitative PCR ($n = 6$). *daw* mutants did not show any significant difference in *shab* expression compared with controls. Error bars represent ± SEM.

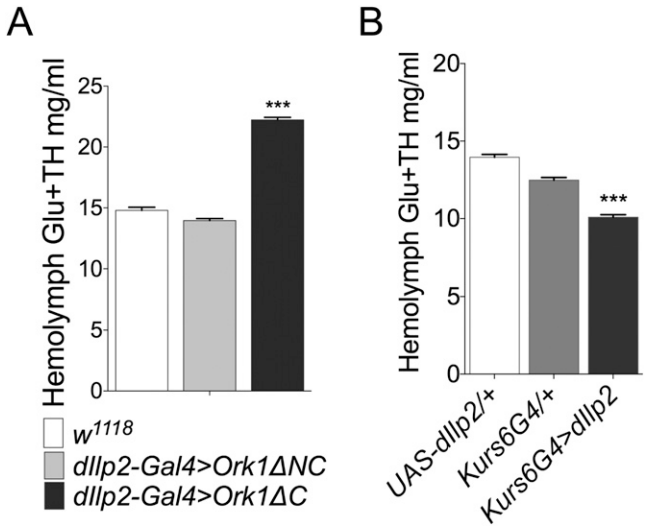

Fig. S6. Verification of tools used to suppress or activate IIS in the larvae (*A*) hemolymph glucose plus trehalose (Glu+TH) concentration of mid–third-instar larvae expressing a potassium channel *Ork1ΔC* in the IPCs ($n = 12$–24). Severely diabetic phenotype in these animals shows that *Ork1ΔC* overexpression in IPCs leads to a severe decrease in IIS. (*B*) The ability of Kurs6Gal4-driven overexpression of dilp2 to increase physiological levels of circulating Dilp2 was tested by assaying for circulating sugar concentration. *Kurs6-Gal4* > *dilp2* was able to significantly reduce circulating sugar concentration in wild-type background ($n =$ 13–16) samples. Error bars represent ± SEM.

GO Category	Number of Genes (Total)	P Value
Genes Up-regulated in *daw*$^{1/11}$ mutants (≥1.3 fold), 560		
Single-organism metabolic process	169 (905)	1.19e-28
Oxidation-reduction process	84 (343)	1.94e-21
Small molecule metabolic process	87 (469)	4.26e-14
Carboxylic acid metabolic process	55 (230)	8.27e-14
Organic acid metabolic process	55 (242)	8.29e-13
Generation of metabolites & energy	31 (104)	7.51e-11
Alpha-amino acid metabolic process	24 (72)	8.61e-10
Cellular amino acid metabolic process	36 (157)	6.84e-9
Electron transport chain	21 (65)	1.87e-8
Lipid metabolic process	34 (204)	3.95e-5
Cellular calcium ion homeostasis	6 (11)	9.21e-5
Myofibril assembly	5 (8)	1.6e-4
Flight	5 (8)	1.6e-4
Fatty acid metabolic process	11 (40)	2.47e-4
Branched chain amino acid transport	3 (3)	5.38e-4
Carbohydrate metabolic process	10 (37)	5.49e-4

GO Category	Number of Genes (Total)	P Value
Genes Up-regulated in *daw*$^{1/11}$ mutants (≥1.3 fold), 560		
Cellular components		
Lipid particle	47 (188)	1.11e-12
Mitochondrial membrane part	29(125)	1.58e-7
Mitochondrial part	56 (359)	1.11e-6
Mitochondrial matrix	16 (56)	5.28e-6
Mitochondrial respiratory chain complex III	6 (12)	1.72e-4
Mitochondrial respiratory chain complex I	11 (39)	1.93e-4
Cytoplasmic part	157 (1528)	4.48e-4
Genes Down-regulated in *daw*$^{1/11}$ mutants (≥1.3 fold), 446		
Small molecule metabolic process	62 (467)	3.13e-8
Oganonitrogen compound metabolic process	55 (391)	2.8e-8
Transmembrane transport	34 (224)	2.68e-6
Organic acid metabolic process	35 (242)	5.85e-6
Microtubule associated complex	32 (352)	2.64e-5
Nucleotide metabolic process	21 (132)	1.14e-4
Glutahione metabolic process	9 (32)	1.44e-4
Amino acid metabolic process	22 (157)	5.08e-4
Single organism bhavior	28 (223)	5.84e-4
Ion transport	24 (184)	8.28e-4

Fig. S7. Table showing gene ontology (GO) classes that were most significantly enriched in up-regulated and down-regulated genes identified in the *daw* mutants.

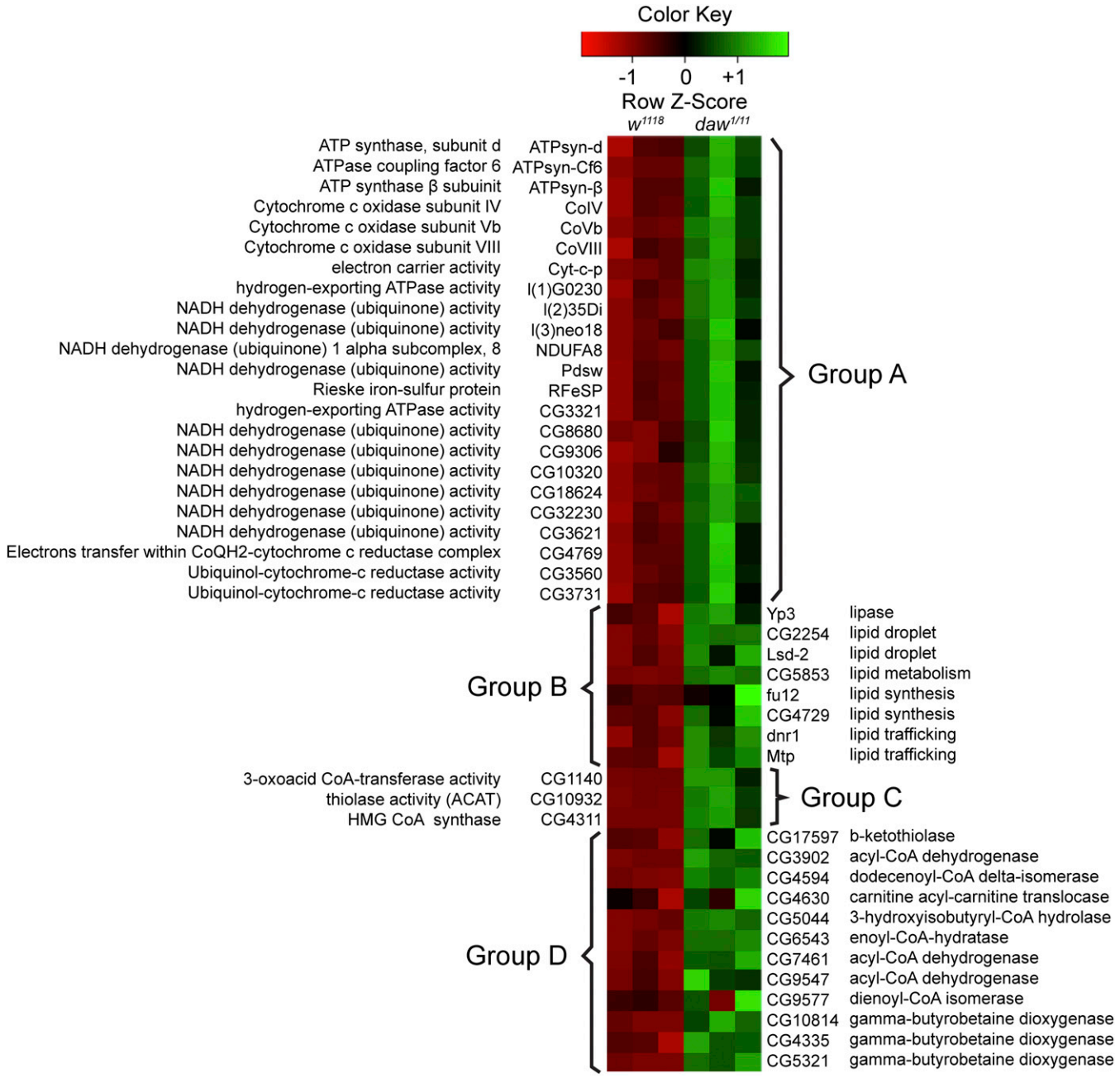

Fig. S8. Heat map showing selected gene groups that were significantly up-regulated in the *daw* mutants. Row Z scores have been color coded with green showing a twofold up-regulation compared with mean value and red twofold down-regulation. Group A shows known and predicted respiratory electron transport chain genes. Group B shows genes involved in lipid mobilization. Group C shows genes involved in ketogenesis. Group D shows genes involved in β-oxidation.

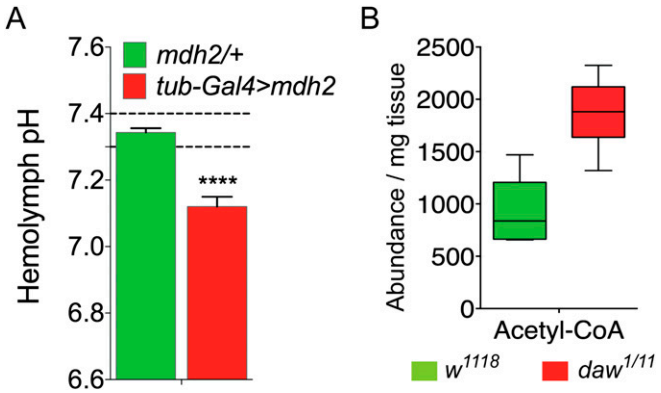

Fig. S9. (*A*) Effect of pan-larval overexpression of *mdh2* on larval hemolymph pH. (*B*) Relative abundance of acetyl-CoA in *daw* mutant and control larvae measured using liquid chromatography/MS.